CIVIL ENGINEERING JOURNAL

Article no. 32

THE CIVIL ENGINEERING JOURNAL 4-2025

STUDY ON MECHANICAL RESPONSE LAW OF SHIELD ASSEMBLY TUNNEL WITH COMPLEX SECTION DURING CONSTRUCTION

Weiming Tao[*1,2], *Xiaoming Liang*[2], *Kun Feng*[2], *Chunfang Lu*[3] *and Chuan He*[2]

1. *China Railway Eryuan Engineering Group Co., Ltd., Chengdu 610031; 478752514@qq.com*
2. *Key Laboratory of Transportation Tunnel Engineering of Ministry of Education, Southwest Jiaotong University, Chengdu 610031; lxmchdedu@163.com, windfeng813@163.com, chuanhe21@163.com*
3. *China Academy of Railway Sciences Corporation Limited; chflu1956@126.com*

Received: 13.06.2024
Received in revised form: 13.06.2025
Accepted: 24.11.2025

ABSTRACT

To investigate the stress and deformation behavior of the mushroom-shaped assembly tunnel, intelligent monitoring and numerical simulation were employed. The mechanical behavior variation during different construction stages, the longitudinal and cross-sectional distribution characteristics, and the deformation control effect of the support on the surrounding rock were analyzed. Comparative analysis assessed the applicability of different excavation methods, and theoretical comparisons discussed the bearing characteristics, providing engineering suggestions. The results indicate that excavation of the lower section has minimal impact on the mushroom head arch but continuously affects the side wall. The arch support of the mushroom head enhances the restraint ability of the lower section support on surrounding rock deformation. In the corner of the wall, the support appears to deviate from the tunnel, where the bolt is compressed. The contact stress of mushroom head increases first, then decreases and then increases from the position near the centroid to both sides. The stress in the transition area between the arch and the straight wall on both sides increases locally, and the stress concentration occurs at the corner of the wall. The deformation of the initial support and the bolt axial force on both sides of the lower section increase first and then decrease from top to bottom, while the law of the contact stress is opposite. Engineering focus should be on arch foot and side wall stress and deformation characteristics for combined flat arch and vertical straight wall support.

KEYWORDS

Large diameter shield, Assembly tunnel with mushroom shape, Intelligent monitoring, Numerical simulation, Mechanical response

INTRODUCTION

For underground engineering, structural safety is particularly important. In the process of construction and operation, the complex stratum environment such as high ground stress and high water pressure and the variable load conditions such as unloading and train load often threaten the safety of underground structures. To ensure the safety of tunnel construction and operation, it is

necessary to clarify the mechanical behavior of underground engineering under different conditions, so as to provide reference for engineering design.

Therefore, many scholars have explored the mechanical behavior of underground engineering under various conditions. The mechanical characteristics of underground engineering are significantly affected by factors such as stratum, groundwater, section shape and support method, so these factors become the main research object. Different complex geological conditions have different effects on the mechanical characteristics of the structure [1]. In layered soft rock, asymmetric deformation of surrounding rock and lining cracking will occur, which is mainly due to the combined action of layered soft rock and shear along the joint plane [2,3]. The dip angle of the strata can influence the surface deformation and stress concentration caused by tunnel excavation [4]. When crossing the fault fracture zone, the supporting structure is subjected to greater surrounding rock pressure [5]. Active faults can cause significant displacement in tunnel structures [6][7]. Moreover, earthquakes are a cause that can activate fault movement [8]. In the soft-hard inclined contact broken stratum with high ground stress, the lining will have asymmetric compression failure [9]. High ground stress also tends to lead to brittle failure of the surrounding rock [10]. To weaken the large deformation of soft rock, the use of double primary support can effectively control the deformation of surrounding rock and weaken the load on the secondary lining [11]. Double primary support can effectively control the large deformation and rheological effect of broken phyllite under high ground stress [12]. The use of prestressed anchorage system can enhance the cohesion of weak surrounding rock and control the deformation of surrounding rock [13]. For the poor stratum of loess, the tunnel is prone to excessive deformation or even lining cracking when constructing the tunnel. π-type SCCS arch can improve the bearing capacity of the structure [14]. In addition, the deformation of underground engineering is also affected by temperature and water. When the periodic temperature changes, it will change the internal force distribution of the structure, accelerate the deformation and failure of the structure, and reduce the bearing capacity of the structure [15]. Water will change the stress distribution of tunnel surrounding rock, which leads to the change of surrounding rock failure mechanism [16]. For double-track super-large cross-section tunnels, the spacing between the two tunnels also has a significant impact on the deformation distribution, crack behavior, and structural internal forces [17]. When the structure is loaded under unfavorable conditions, the bearing capacity of the structure can also be improved by prestressed composite lining [18]. The bearing capacity of the composite structure is obviously better than that of the double-shell structure [19]. Steel fiber significantly improves the structural toughness and bearing capacity [20]. Structures reinforced with a combination of steel fibers and rebar exhibit more outstanding performance [21]. In addition to the formation conditions, the shape of the section will also affect the mechanical characteristics of underground engineering. Through the numerical simulation method, it is very convenient to realize the mechanical response of excavation with different cross-section shapes [22]. The influence mechanism of opening shape on rock failure can be explored by processing openings of different shapes and sizes on rock blocks [23]. A full-scale ring test shows that the bearing capacity and failure characteristics of the quasi-rectangular shield tunnel structure are significantly different from those of the circular structure [24]. Bolt mortise, tenon joint and interior column can effectively improve the bearing capacity of rectangular tunnel structure [25] [26]. By optimizing the shape of the tunnel section, the stress concentration can be reduced and the structural stress can be improved [27].

The existing research mainly focuses on the influence of stratum conditions, support methods and section forms on the mechanical behavior of underground engineering. Among them, the section forms are mostly circular, rectangular, horseshoe-shaped and other conventional sections, and there are few studies on more complex sections such as mushroom-shaped sections. To clarify the mechanical response law of mushroom-shaped complex section, this study relies on the shield tunnel of Chongqing Yangtze River Railway to explore the deformation control characteristics of surrounding rock in large-section mushroom-shaped shield assembly tunnel Then, the mechanical characteristics of the supporting structure during the construction process were analyzed, and then the mechanical characteristics of the structure were discussed and optimized.

Existing research has explored the mechanical behavior of tunnels under various conditions, with tunnel cross-sections typically being conventional shapes such as circular or horseshoe-shaped. The size and shape of the cross-section significantly influence the stress and deformation patterns of the tunnel. Due to geographical constraints, the shield assembly tunnel in Chongqing Yangtze River Tunnel employs a mushroom-shaped cross-section, with an arched upper section and a rectangular lower section. The cross-section is the largest among existing shield assembly tunnel, resulting in more construction procedures and increased construction difficulty. The span of the upper section is significantly larger than that of the lower section. Unlike conventional cross-sections such as circular or horseshoe-shaped ones, this cross-section features multiple corners prone to stress concentration. Additionally, the vertical side walls of the lower section are susceptible to lateral squeezing from the surrounding rock. The mechanical characteristics of this complex cross-section are intricate and under-researched. To address this, this study, based on the Chongqing Yangtze River Tunnel, uses intelligent monitoring and numerical simulation to investigate the deformation control characteristics of the surrounding rock in large-section mushroom-shaped shield assembly tunnel. It also analyzes the mechanical characteristics of the support structure during construction using theoretical methods and discusses and optimizes the structural mechanical characteristics. This study is the first to explore the interaction mechanism between support and surrounding rock in large-section mushroom-shaped assembly tunnel during construction, providing a reference for similar projects.

ENGINEERING OVERVIEW AND DESIGN

Engineering overview

Chongqing Yangtze River Tunnel is a railway line control project from Chongqing-Qianjiang, and the river-crossing section is constructed by shield method. The tunnel is a double-track extra-long tunnel, which is managed according to the Class I high-risk tunnel and is one of the 12 key projects on the whole line. The outer diameter of the shield segment is 12.2 m, which is a large-section river-crossing tunnel. The tunnel passes through important areas such as Yuzhong Peninsula urban area, Yangtze River and Nanping urban area. Yuzhong Peninsula urban area and Nanping urban area are shallow hilly landforms, located in the urban area. The strata in the tunnel are mainly sandstone and mudstone, and locally limestone and dolomite.

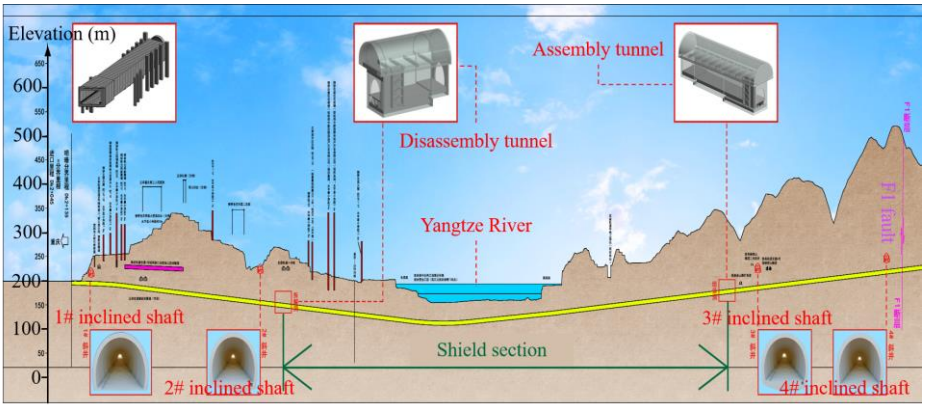

Fig. 1 – Longitudinal section line diagram of Chongqing Yangtze River Tunnel

Assembly tunnel design

The starting position of the shield is located inside the mountain, and the surface altitude is significantly higher than that of the river section. This makes the location does not have the conventional launching conditions, so the design adopts the scheme of large buried depth assembly tunnel shown in Figure 2. The starting and ending mileage of the assembly tunnel is DK7+650~DK7+700, and the buried depth reaches 149.23 m. The assembly tunnel is designed as

a two-stage structure: a transition section (15m, DK7+685~DK7+700) and a sinking section (35m, DK7+650~DK7+685). The section of the tunnel is mushroom-shaped, the upper section is mushroom head, and the lower section is rectangular. The shield components are transported to the assembly tunnel through the tunnel of the mining method section, and then the shield hoisting, trolley assembly, cutterhead installation and shield assembly are carried out. To meet the hoisting requirements, the maximum span of the tunnel is 25.54 m, and the maximum height is 29.96 m, which is the shield assembly tunnel with the largest section.

Fig. 2 – Assembly tunnel

The mushroom head of the assembly tunnel and the lower section of the sinking section are excavated in four steps, and the lower section of the transition section is excavated in three steps. The specific order is shown in Figure 3. Each excavation section is excavated to the maximum longitudinal length of the tunnel, and then the next section is constructed. After the excavation of each section is completed, spray anchor support and temporary support are applied in time. The bolt in mushroom head adopts φ25 combined hollow bolt, and the length of 4.5 m and 6.0 m is alternately arranged in plum shape. The bolt in lower section adopts φ32HRB400 mortar bolt.

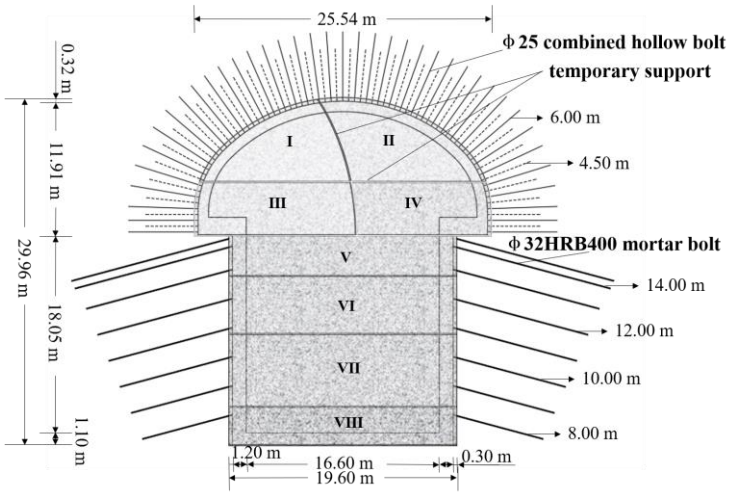

Fig. 3 – Section shape and construction design

INTELLIGENT MONITORING OF MECHANICAL BEHAVIOR IN ASSEMBLY TUNNEL

Monitoring scheme

The intelligent monitoring system is used to monitor the deformation of the initial support, contact stress and bolt axial force of the assembly tunnel, so as to clarify the variation law of the mechanical behavior of the support structure during the construction process. The mileage of the

monitoring section in this study is DK7+670, and the arrangement of monitoring elements and measuring points is shown in Figure 4. A1~A5 are deformation monitoring, of which A1 is settlement monitoring, the rest are convergence monitoring, and the monitoring instrument is laser deformation measuring instrument. B1~B5 are the contact stress monitoring of the initial support and the surrounding rock, and the monitoring instrument is the earth pressure box. C1~C5 is the monitoring of the bolt axial force, and the monitoring instrument is the bolt axial force meter. The deformation monitoring results are collected by the deformation acquisition box, and the contact stress and bolt axial force are collected by the stress acquisition box, and then uploaded to the data monitoring platform through wireless transmission to realize real-time monitoring.

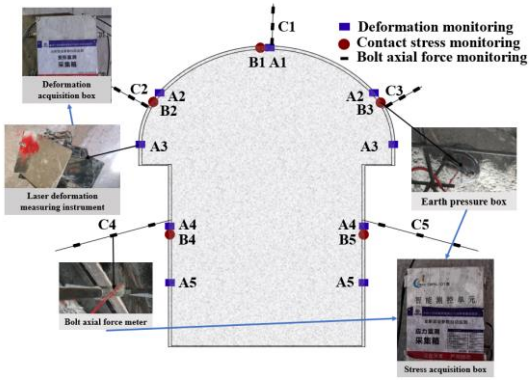

Fig. 4 – Installation of field monitoring elements and arrangement of measuring points

Diachronic characteristics of mechanical behavior in assembly tunnel

Figure 5 is the variation law of the initial support deformation during construction. The secondary lining in the mushroom head is applied before the excavation in the lower section, so the deformation in the mushroom head only analyzes the excavation process in the upper section. In addition, the deformation in the direction towards the tunnel is positive, and the deformation in the direction away from the tunnel is negative. It can be seen from the diagram that the vault (A1) settlement increases rapidly in the excavation of section II, and increases with the subsequent excavation but the increase is small. Arch foot (A2) and mushroom head side wall (A3) all produce convergence deformation deviating from the tunnel. The convergence deformation in arch foot (A2) increases during the excavation of section I and II, and decreases during the excavation of section III. This is because the section span increases after the excavation of section II, and the section height increases after the excavation of section III. The convergence deformation in the mushroom head side wall (A3) continues to increase, which is due to the increase of the IV section span. After the excavation of the section and the next section, A4 and A5 are deformed towards the tunnel, which is less affected by the subsequent excavation.

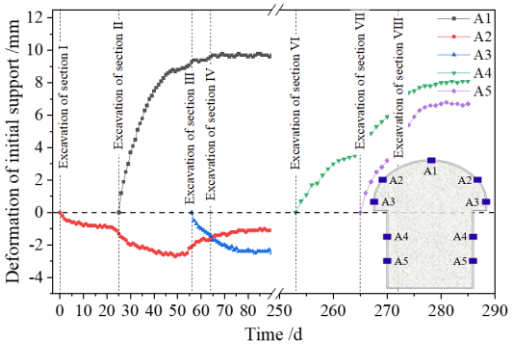

Fig. 5 – Deformation duration curve of initial support

Figure 6 is the change law of contact stress during construction. It can be seen from the diagram that the vault (B1) gradually increases after the excavation of the II section, and slowly

decreases in the subsequent section excavation. After the excavation of the section and the next section, the contact stress of the arch foot (B2, B3) increases significantly, and decreases rapidly after the excavation of the lower section. This is because the horizontal deformation of the surrounding rock squeezed by the arch foot decreases after the excavation of the lower section, and the vertical deformation towards the tunnel increases. After the excavation of the lower section, the contact stress of B2 and B3 changes slightly. The contact stress of B4 and B5 increases gradually only after the excavation of their section, and decreases rapidly after the subsequent excavation. Because the height of the section increases, the horizontal deformation of B4 and B5 increases, and the contact degree between the surrounding rock and the support decreases.

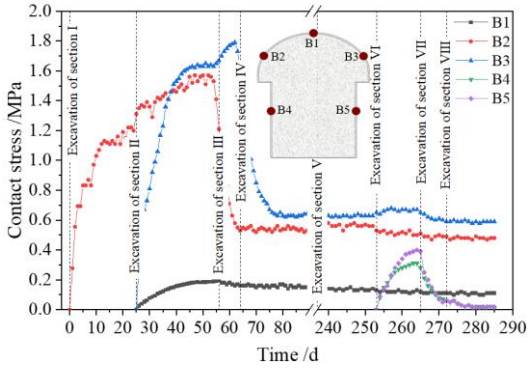

Fig. 6 – Contact stress duration curve

Figure 7 shows the variation law of the maximum bolt axial force during construction. Except for arch feet (C2, C3), the variation law of axial force at other positions is basically consistent with the deformation of initial support, and the excavation of lower section has no obvious influence on the axial bolt force in mushroom head. C2 and C3 are in a state of compression before the excavation of the lower section, and gradually become a state of tension after the excavation of the lower section. Because the horizontal deformation in the arch foot away from the surrounding rock is reduced, the vertical settlement is increased.

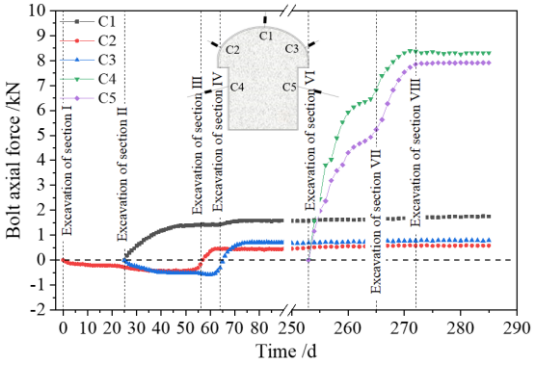

Fig. 7 – Bolt axial force duration curve

NUMERICAL SIMULATION OF MECHANICAL BEHAVIOR IN ASSEMBLY TUNNEL

Monitoring scheme

The strata where the assembly tunnel is located are mainly mudstone and sandstone. The sandstone is the main stratum, and the overlying thickness of the vault is about 74.23 m. The mudstone is the overlying stratum of sandstone, and the thickness is about 75.00 m. The Mohr-Coulomb constitutive model is one of the most widely used strength theories in geotechnical engineering. It is simple in form and effectively describes the mechanical behavior of rock and soil. It is widely used in numerical simulations of geotechnical engineering projects, including tunnels and

excavations. Geological surveys indicate that the strata in this project are relatively homogeneous. Therefore, both mudstone and sandstone adopt Mohr-Coulomb constitutive model. After the excavation of the tunnel, the support mainly includes initial support, temporary support, bolt and secondary lining. The model is shown in Figure 8. The stratum, the temporary support, the initial support and the secondary lining are solid elements, which are elastic materials. To more accurately simulate the interaction between the strata and the structure, contact elements have been employed to model these interfaces. Contact elements can effectively handle the contact, friction, and separation behaviors between the strata and support structures, thereby more realistically reflecting the mechanical behavior in actual engineering applications. The parameters of the interface mainly include the normal stiffness and shear stiffness, which can be calculated using Eq. (1). The implementation of the bolts is accomplished by utilizing the built-in cable elements. These elements, specifically designed for simulating rod-like structures, effectively model the stretching behavior of bolts under load and their interactions with the surrounding medium. Specifically, the cable elements transmit both axial and shear forces and account for the frictional and cohesive interactions between the bolt and the surrounding rock, thus faithfully reproducing the mechanical function of the bolts within the numerical model. The numerical simulation construction process is consistent with the actual situation. The strata parameters and support parameters are based on geological exploration data and engineering design, as shown in Table 1 and Table 2.

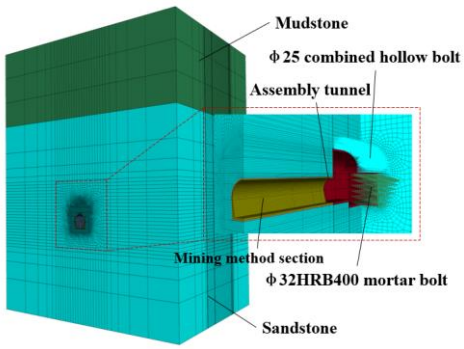

Fig. 8 – Numerical model

$$k_n = k_s = 10 \cdot \max[\frac{K_r + \frac{4}{3}G_r}{\Delta z_{\min}}] \quad (1)$$

Where kn is the normal stiffness, ks is the shear stiffness, Δzmin is the minimum size of the adjacent regions in the normal direction of the interface, Kr is the bulk modulus, and Gr is the shear modulus.

Tab. 1 - Strata parameters

Strata	Density /（kg/m3）	Cohesion /MPa	Internal friction angle /°	Elastic modulus /GPa	Poisson ratio
Mudstone	2520	2.10	38.31	2.367	0.32
Sandstone	2456	6.29	41.02	6.804	0.23

Tab. 2 – Supporting parameters

Type	Thickness /m		Elastic modulus /GPa	Poisson ratio
Initial support	Mushroom head	0.32	28.0	0.2
	Lower section	0.30		
Temporary support	0.11		28.0	0.2
Secondary lining	Mushroom head	0.9	30.0	0.2
	Lower section	1.2		

Longitudinal mechanical characteristics of assembly tunnel

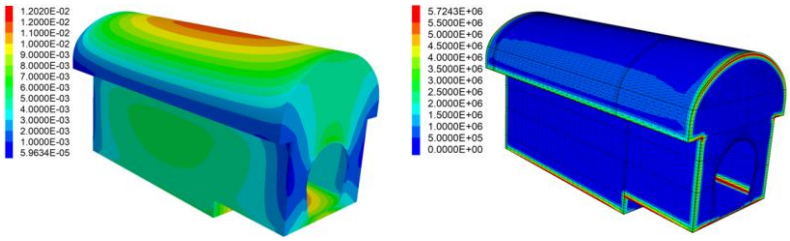

(a) Deformation of initial support *(b) Contact stress*

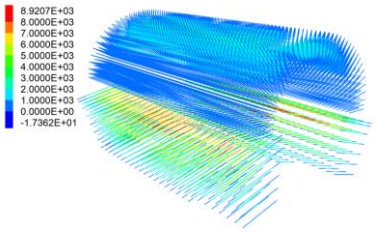

(c) Bolt axial force

Fig. 9 – Longitudinal mechanical characteristics of assembly tunnel

Control effect of surrounding rock stability

Figure 10 is the deformation law of surrounding rock with or without support. Regardless of whether there is support or not, the deformation of vault surrounding rock is mainly vertical settlement. The deformation of the surrounding rock from the vault to the wall corner of the mushroom head gradually decreases, and the deformation direction gradually changes from vertical settlement to horizontal settlement. The bottom of the tunnel is mainly uplifted. The deformation in the upper part of the side wall in the lower section is significantly larger than that of the lower part without support, and the deformation in the middle part of the side wall is larger after support. because after the support is applied, the vertical effect of the upper load on the arch structure and the horizontal thrust of the squeezed soil are transmitted downward through the support structure, but the transmission effect is gradually weakened.

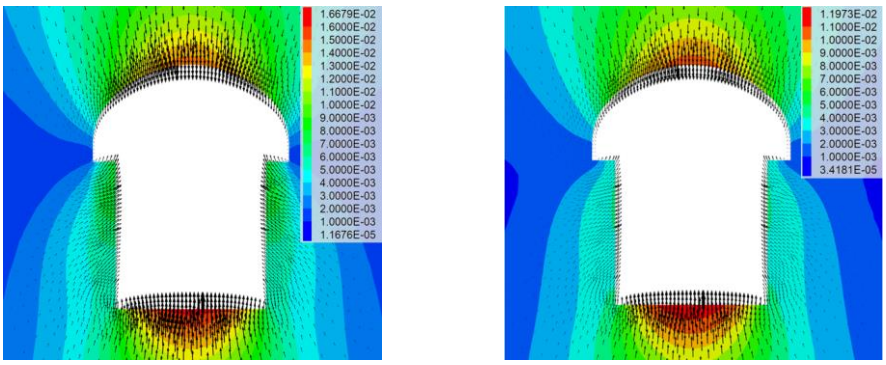

(a) Without support (b) With support

Fig. 10 – Surrounding rock deformation

To clarify the effect of support on the deformation control of surrounding rock, the deformation of typical positions was extracted, and the deformation control rate (the ratio of deformation change after support to unsupported deformation) was analyzed, as shown in Table 3. After support, the

deformation control rate of mushroom head increases first and then decreases from vault to arch foot. When there is no support, the bearing arch formed by the surrounding rock itself has a strong ability to resist deformation at the arch foot, so the deformation control rate at the arch foot after support is relatively low. The deformation control rate of the lower section gradually decreases from top to bottom, which indicates that the position of the larger deformation in the side wall moves down. On the whole, the deformation control rate of mushroom head is less than that of the lower section. On the one hand, it is due to the better self-stabilizing ability of the mushroom head arch structure when there is no support. On the other hand, the arch structure after support will enhance the constraint ability of the lower structure to the deformation of the surrounding rock.

Tab. 3 - Control effect of surrounding rock deformation

Location		Deformation value /mm		Deformation control rate /%
		Without support	With support	
Mushroom head	Vault	14.65	10.57	27.85
	Spandrel	10.17	7.08	30.38
	Arch foot	2.22	1.92	15.31
Lower section	Upper part	7.53	4.06	46.08
	Middle	6.31	3.99	36.77
	Lower part	5.30	3.75	29.25
	Bottom	16.68	11.97	24.24

DISTRIBUTION LAW OF CROSS-SECTION MECHANICAL CHARACTERISTICS IN ASSEMBLY TUNNEL

Deformation of initial support

Figure 11 shows the distribution law of initial support deformation in different excavation stages of mushroom head. After the excavation of each section, the arch is dominated by the vertical deformation towards the tunnel, and the lower wall corner is dominated by the horizontal deformation away from the tunnel. After the excavation of section II, the span of the tunnel increases by about one time, and the vertical deformation in the arch and the horizontal deformation in the corner of section I increase significantly. This shows that as the span increases, the vertical deformation in the arch increases, and the squeezing degree of the wall corner on the surrounding rock will also be aggravated. After the excavation of the section IV, compared with the excavation of the section II, the section height increases, the vertical deformation of the arch increases, and the horizontal deformation of the support on both sides decreases. The deformation at the corner of section I is 2.51 mm and 2.45 mm respectively, and the numerical difference is not significant, but the former is mainly horizontal deformation, and the latter is mainly vertical deformation. This means that the increase of the section height will weaken the extrusion degree of the structure towards the surrounding rock.

When the excavation section is an asymmetric structure, such as the excavation of sections I and III, the vertical deformation near the center of the excavated section is greater than the deformation away from the centroid, and the horizontal deformation away from the centroid will increase. After the excavation of section III, the deformation of the corner in section II, which is mainly horizontal displacement, is 3.03 mm, while the deformation of the corner of section II is 2.54 mm. When the excavation section is a symmetrical structure, the support deformation is also symmetrically distributed.

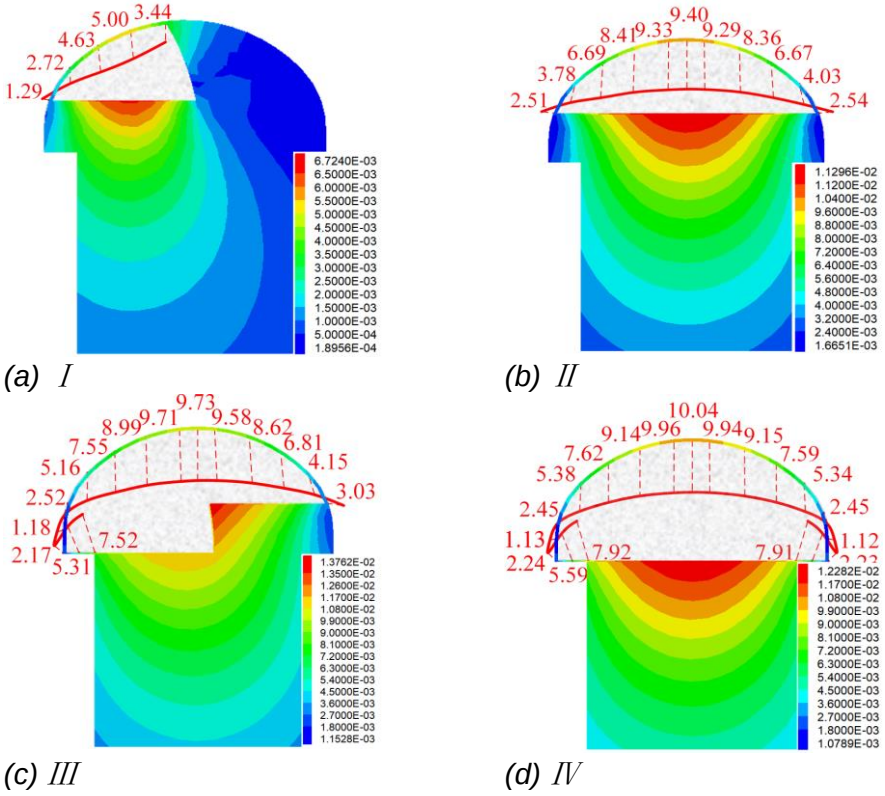

Fig. 11 – Initial support deformation during excavation of mushroom head (unit: mm)

Figure 12 is the distribution law of the deformation at different excavation stages of the lower section. The support of the lower section is a straight wall, which directly bears the horizontal extrusion of the surrounding rock on both sides. However, after the excavation of section V, the side wall does not deform horizontally towards the tunnel, but has a horizontal displacement slightly deviating from the tunnel. This shows that the thrust of the squeezed surrounding rock produced by the mushroom head support also has a significant impact on the lower section support. After the excavation of section VI, the side wall has a horizontal displacement towards the tunnel, which indicates that the horizontal thrust effect of the mushroom head support is weaker than the direct effect of the surrounding rock on the side wall. With the increase of section height, the direct effect of surrounding rock on the side wall is more significant, and the horizontal deformation of the side wall increases first and then decreases from top to bottom. In addition, the excavation of the lower section has little effect on the deformation of the mushroom head arch, and the vertical displacement increases slightly. As the section height increases, the side wall of the mushroom head is significantly affected, and the deformation from the tunnel gradually changes to the deformation towards the tunnel.

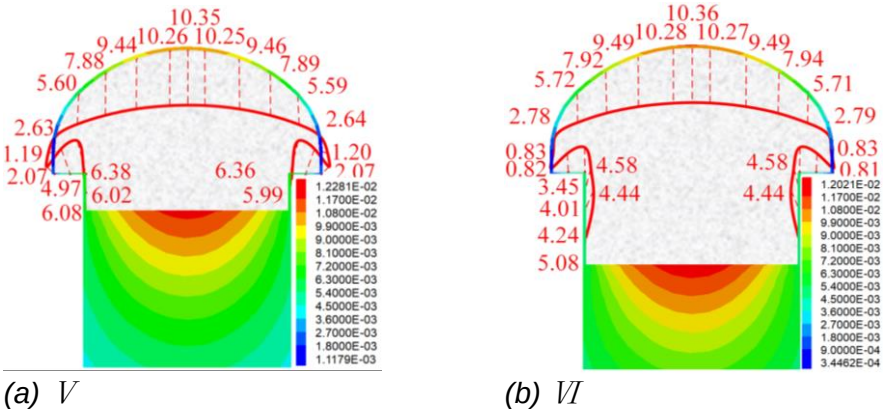

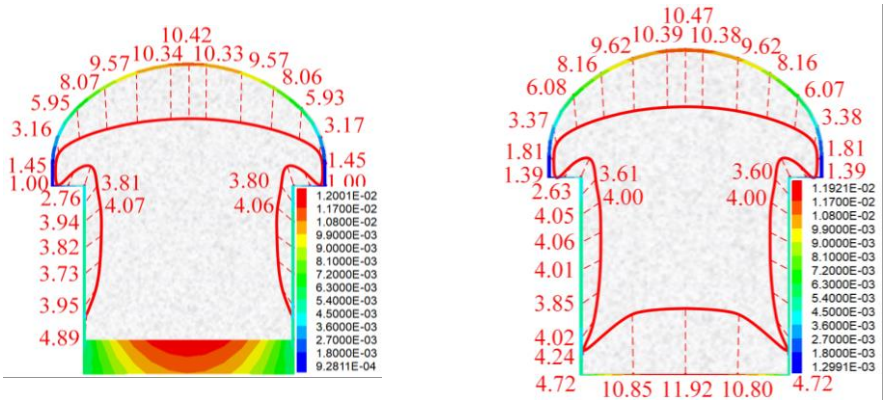

(c) Ⅶ *(d) Ⅷ*

Fig. 12 – Initial support deformation during excavation of lower section (unit: mm)

Contact stress

Figure 13 shows the distribution law of contact stress between initial support and surrounding rock at different excavation stages of mushroom head. On the whole, the contact stress of the arch is small, because the arch has obvious deformation towards the tunnel, and the stress release is significant. There are sharp corners in the support of each excavation section, resulting in obvious stress concentration. On the one hand, it is because there is a sudden change in the shape of the support at these positions. On the other hand, it is because these positions produce deformation that deviates from the tunnel and squeezes the surrounding rock. The increase of the cross-section span will further release the stress of the arch and increase the stress of the corner. After the excavation of section II, the arch stress of section I decreases, while the corner stress increases from 3.93 MPa to 4.55 MPa. The height of the section increases, and then the stress of the arch and both sides decreases.

When the section is eccentrically compressed, the stress near the centroid of the excavated section is less than the stress away from the centroid. When the section is a symmetrical structure, the stress is also symmetrically distributed, and it increases first, then decreases and then increases from the vault to both sides. The stress of the arch foot increases, indicating that the horizontal thrust effect is the most significant here, and the horizontal thrust effect is weakened on the side wall.

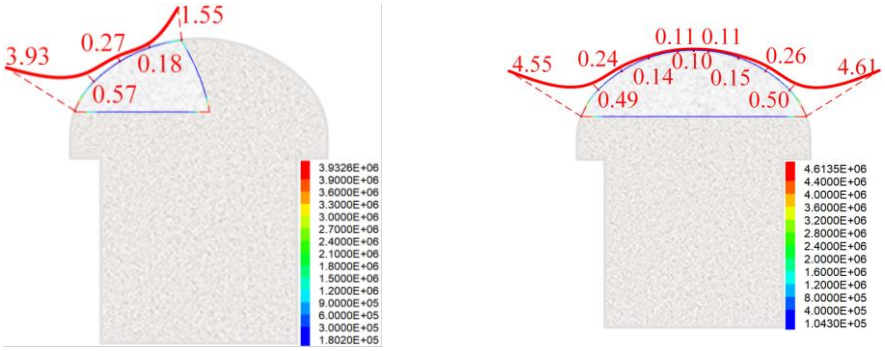

(a) Ⅰ *(b) Ⅱ*

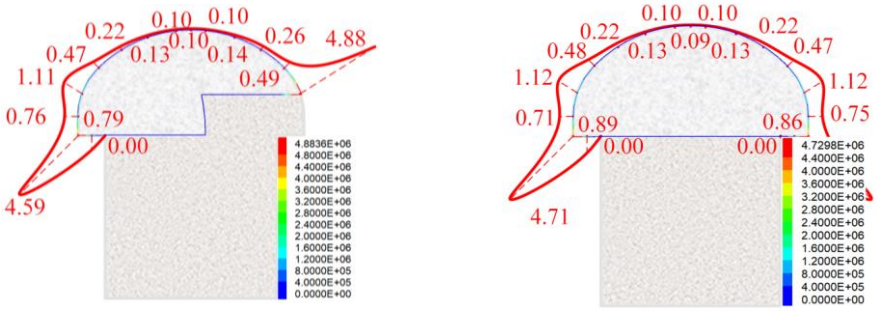

(c) III *(d) IV*

Fig. 13 – Contact stress during excavation of mushroom head (unit: MPa)

Figure 14 is the distribution law of contact stress in different excavation stages of lower section. In the excavation of the lower section, the height of the section increases, which has little effect on the stress of the arch of the mushroom head, and the influence on both sides is slightly larger. After the excavation of section V, the horizontal thrust of mushroom head is still obvious, and the stress on both sides increases. Subsequently, the height of the section continues to increase, and the stress on both sides of the mushroom head gradually decreases due to the deformation of the lower section towards the tunnel. The stress on both sides of the lower section decreases first and then increases from top to bottom, and there is a non-compression state in the middle. Because the support on both sides of the lower section is a straight wall, and the upper and lower ends are constrained by horizontal support, and the horizontal deformation is small. However, the horizontal deformation in the middle is significant, and the surrounding rock at the bottom has a squeezing effect on the straight wall, which further increases the bending degree of the middle part of the straight wall towards the tunnel, and weakens the mutual squeezing effect between the partial support and the surrounding rock.

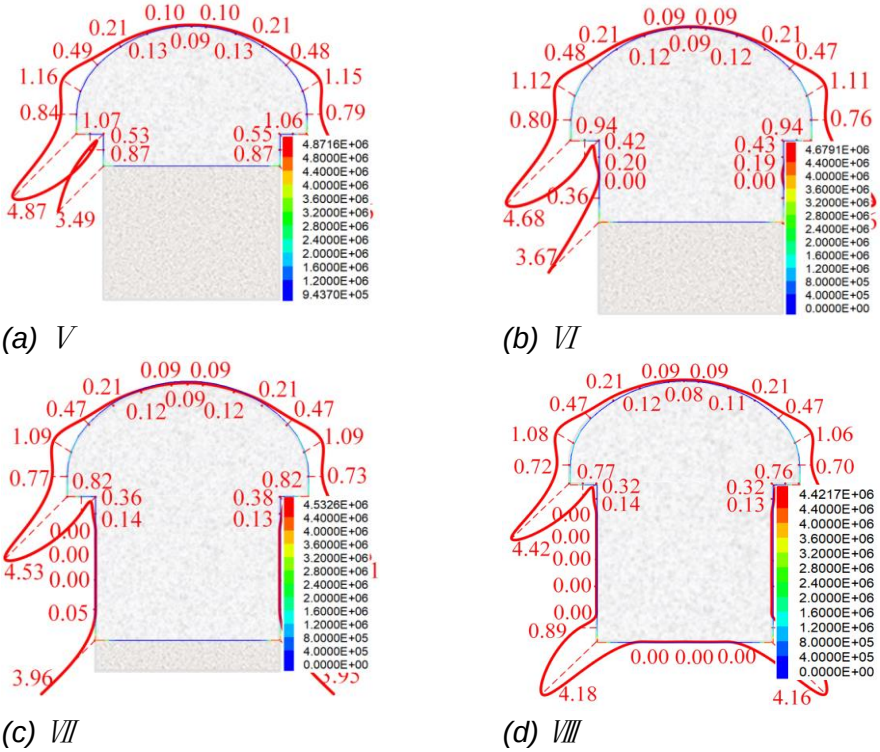

(a) V *(b) VI*

(c) VII *(d) VIII*

Fig. 14 – Contact stress during excavation of lower section (unit: MPa)

Bolt axial force

Figure 15 shows the distribution law of bolt axial force in different stages of mushroom head excavation. The arch bolt is in a tensile state, and the lower bolt is in a compressive state. This is because the arch produces a displacement pull bolt toward the tunnel, and the bottom produces a displacement compression bolt that squeezes the surrounding rock. Along the length direction of the bolt, the maximum axial force of the bolt appears in the middle of the bolt, which is the main action area of the bolt. Along the section direction, the maximum bolt axial force is located in the middle of the section and gradually decreases to both sides. The bolt axial force is positively correlated with the span and height of the section.

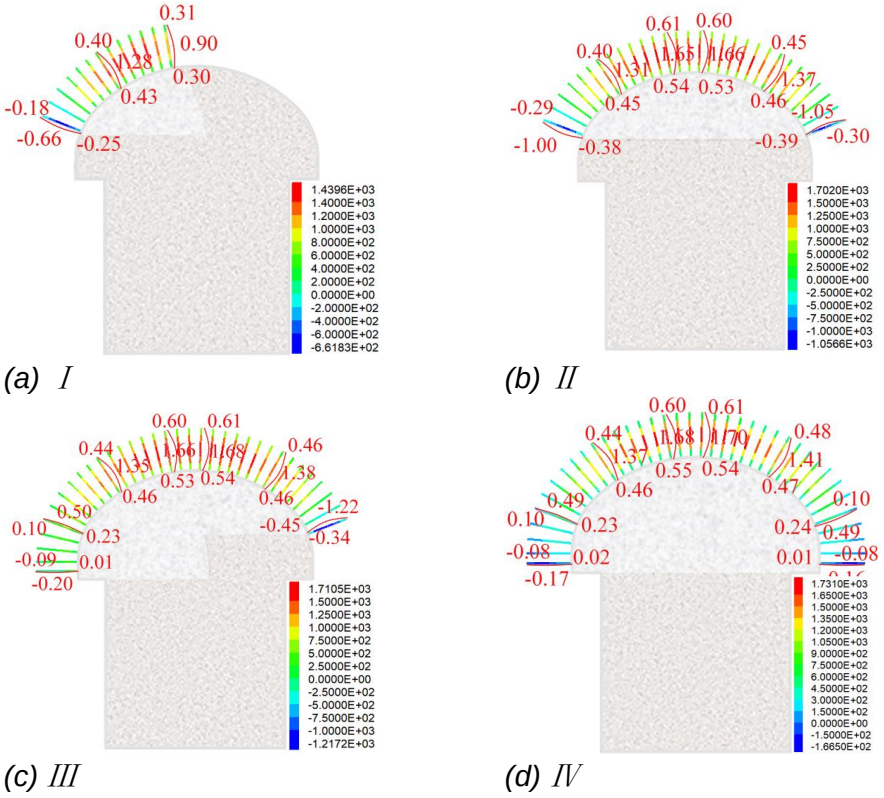

Fig. 15 – Bolt axial force during excavation of mushroom head (unit: kN)

Figure 16 is the distribution law of bolt axial force in different excavation stages of lower section. As the excavation height of the lower section increases, the bolt axial force on both sides of the mushroom head gradually increases, and the lower compression bolt gradually becomes a tension bolt. The bolt axial force in the lower section increases first and then decreases from top to bottom, and the upper part in the lower section bolt is generally greater than the lower part. This is because the horizontal deformation of the upper part towards the tunnel is significantly larger than that of the lower part, and the effect of the bolt is more significant.

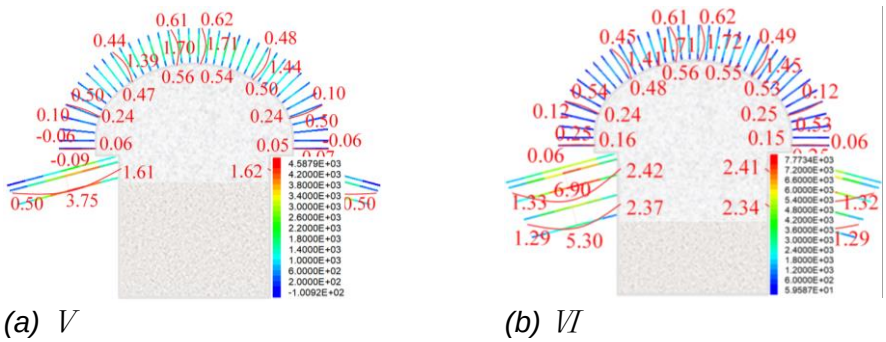

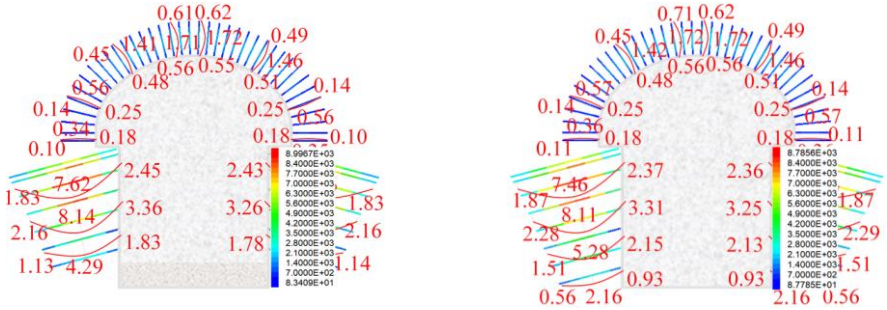

(c) Ⅶ (d) Ⅷ

Fig. 16 – Bolt axial force during excavation of lower section (unit: kN)

DISCUSSION AND SUGGESTIONS

Excavation method

With reference to similar large-section tunnel projects under the same geological conditions, this project designed two upper section excavation methods: the center diaphragm (CD) method and the double side heading (DSH) method (Figure 17). To improve the efficiency, this project adopts the CD method with less steps. To clarify the adaptability of these two methods in this project, the mechanical response characteristics of the DSH method are further compared, as shown in Figure18.

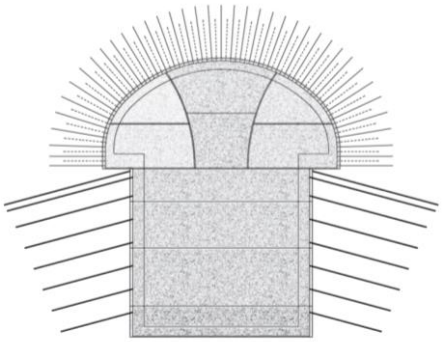

Fig. 17 – Double side heading method

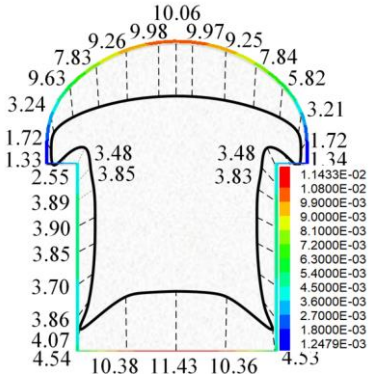

(a) Deformation of initial support

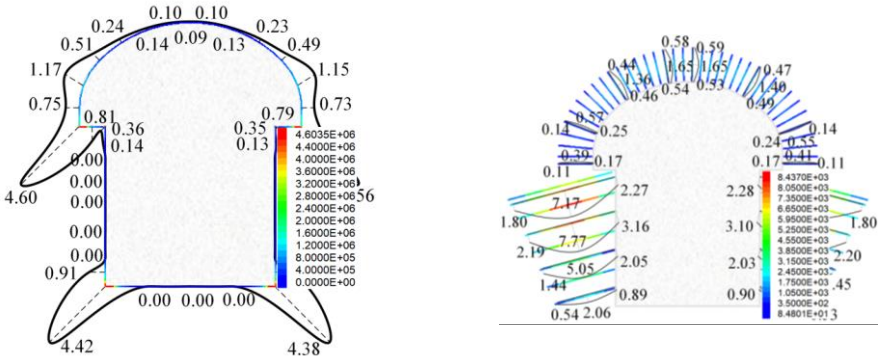

(b) Contact stress *(c) Bolt axial force*

Fig. 18 – Mechanical characteristics of DSH method

Adopting the DSH method, the deformation of the initial support and the bolt axial force are relatively small, but the contact stress increases. This is because the excavation section of each process in the DSH method is small, and the initial support of each section is closed in time after excavation, so that the deformation is better controlled, and the smaller deformation also weakens the effect of the bolt. At the same time, the stress release is also weakened, so that the initial support is subjected to greater stress, and the stress concentration is more significant. As far as the deformation of the initial support is concerned, the method in this paper and the DSH method are reasonable, indicating that both methods meet the construction requirements. In similar projects, if the deformation control requirements are higher, the DSH method can be preferred. However, the DSH method has many processes, slow construction and high cost. Similar to this project, the CD method can be preferred when the deformation control is within the safe range.

Load model

Based on the above analysis, the large deformation of the assembly tunnel is located at the vault and the arch bottom, which is the main position for the stress release of the surrounding rock. The local stress at the transition position from the mushroom head arch to the straight wall on both sides is large, and significant stress concentration occurs at the wall corner. Due to the complex section form, the load model of the assembly tunnel is different from that of the conventional tunnel section. Therefore, the results of field monitoring and numerical simulation of contact stress are compared with the theoretical calculation. Due to the large buried depth of the assembly tunnel, the theoretical method adopts the 'Code for Design of Rai1way Tunnel' (Eqs. (2)~(5)) and the Protodyakonov's theory (Eqs. (6)~(7)). The horizontal load in the Protodyakonov's theory calculation adopts the Rankine formula (Eqs. (8)~(9)), and the calculation model is shown in Fig. 19.

$$q = \gamma h \tag{2}$$

$$h = 0.45 \times 2^{s-1} \omega \tag{3}$$

$$\omega = 1 + i(B-5) \tag{4}$$

$$e = kq \tag{5}$$

where q is the vertical load; γ is the weight of surrounding rock; B is the tunnel span; i is the coefficient related to B; e is horizontal load; k is the horizontal load coefficient.

$$q = \gamma H \tag{6}$$

$$H = \frac{L}{2f} = \frac{B/2 + h_1 \tan\varphi}{f} \tag{7}$$

$$e = K_a(q + \gamma h_2) \tag{8}$$

$$K_a = \tan^2(45 - \varphi/2) \tag{9}$$

where H is the equilibrium arch height; L is the width of collapse arch; f is the rock firmness coefficient; h1 is the buried depth of the tunnel ;Ka is the Rankine earth pressure coefficient; h2 is the depth of the straight wall; φ is the internal friction angle of surrounding rock.

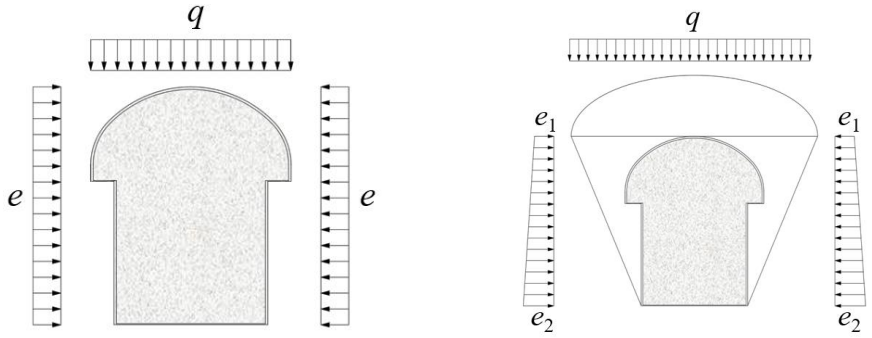

(a) Code for Design of Rai1way Tunnel

(b) Protodyakonov's theory

Fig. 19 – Load mode of theoretical method

Figure 20 is the surrounding rock pressure obtained by different methods, and the horizontal axis is the distance from the vault to the lower section wall corner. Based on the theoretical method, the surrounding rock pressure in the arch shows a trend of increasing first and then decreasing. However, the results of field monitoring and numerical simulation gradually increase. The numerical simulation and field monitoring results near the arch foot are larger, which are significantly higher than the theoretical method. The arch of the mushroom head is a large-span arched flat structure. Under the action of the upper load, the reverse thrust will be generated to squeeze the soil, and the effect at the arch foot is the most obvious. Compared with the circular and horseshoe-shaped sections, the vault stress of the flat elliptical section is smaller, and the stress of the upper half arch foot is larger. In addition, the smaller the flat rate is, the more significant it is, and the stress concentration occurs at the arch foot. This is the main reason why the difference between theoretical method, numerical simulation and field monitoring is more and more significant when the distance from the arch foot is closer. The surrounding rock pressure of the transition section from the arch foot to the side wall in the mushroom head decreases gradually, because the transition section with smaller curvature and vertical direction tends to produce deformation deviating from the surrounding rock, which weakens the effect of the reverse thrust of the arch structure continuing to transfer downward. In addition, the corner of the mushroom head and the lower section have significant stress concentration, and the larger value affects the comparison of the remaining positions, so it is not reflected in Figure 20. In the numerical simulation, the side wall of the lower section is not affected by the pressure of the surrounding rock except for the upper and lower ends. The field monitoring results are also significantly smaller, which is significantly different from the theoretical calculation results. This is because the upper and lower ends of the side wall are subjected to horizontal and vertical loads and are constrained. The middle part of the side wall has a large degree of deflection towards the tunnel, and the degree of squeezing the surrounding rock is weak. Based on experience and Rankine's formula, the characteristics of side wall under load and constraint cannot be considered, so there are differences with the simulation and measured results.

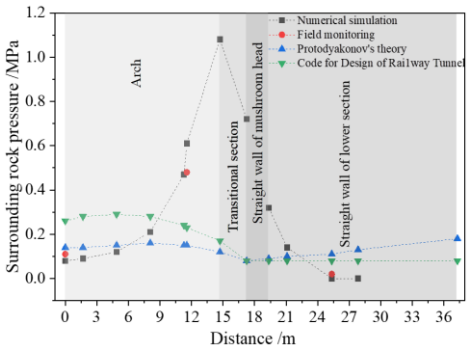

Fig. 20 – Comparison of surrounding rock pressure

Engineering proposal

Numerical simulation and field monitoring show that the stress at the arch foot and below the mushroom head is significantly greater than the theoretical results. To ensure the safety of the structure, support should be strengthened in engineering design, and monitoring should be strengthened in construction. Because the structure needs long-term bearing stress, it is appropriate to optimize the corner shape, such as optimizing the right angle into a rounded corner to weaken the stress concentration. Figure 21 is the distribution characteristics of structural mechanics after simulation optimization. The vertical deformation of the mushroom head decreases slightly, the horizontal displacement of the upper part on both sides of the lower section increases slightly, and the horizontal displacement of the lower part decreases slightly. Therefore, the contact stress of mushroom head increases slightly, and the bolt axial force decreases. The contact stress on the upper part of the lower section decreases, the bolt axial force the increases, and the axial force of the lower bolt decreases. The corner of the wall is transitioned from the corner, the displacement increases, and the contact stress decreases significantly, indicating that the corner can significantly weaken the stress concentration of the corner.

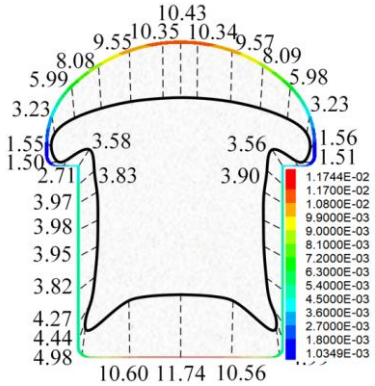

(a) Deformation of initial support

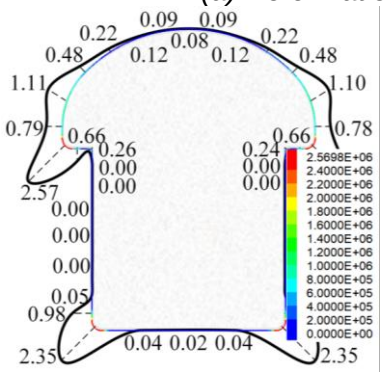

(b) Contact stress

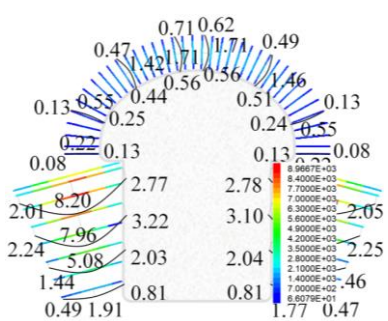

(c) Bolt axial force

Fig. 21 – Mechanical characteristics of optimized section

In addition, the middle part of the side wall in the lower section is less loaded in the simulation and measurement. This does not mean that the structure is safe, but there is a possibility that the structure is in an unfavorable state due to excessive deflection. For the large buried deep straight wall, the structural deflection deformation should be focused on, and grouting reinforcement measures should be taken when necessary. Prestressed anchor cable, bolt encryption and other strengthening measures can also be used in the design.

CONCLUSION

Based on the Chongqing Yangtze River Tunnel, the mechanical behavior variation law and section distribution characteristics of the large-section mushroom-shaped shield assembly tunnel in different construction stages were explored. The specific conclusions are as follows:

(1) The excavation of the lower section has little effect on the mechanical behavior of the mushroom head arch. The influence on the straight walls on both sides is slightly larger, and the influence gradually increases with the excavation depth.
(2) The deformation control rate of the lower section is higher than that of the mushroom head, and the larger deformation position in the lower section moves down after the support, indicating that the mushroom head support can enhance the constraint ability of the lower section support to the surrounding rock deformation, and the enhancement effect gradually weakens downward.
(3) The deformation of the initial support and the bolt axial force the are positively correlated with the the tunnel span. The vertical deformation of the initial support and the bolt axial force are positively correlated with the tunnel height, and the horizontal deformation is negatively correlated with the tunnel height. The contact stress of mushroom head arch is negatively correlated with the tunnel span, and the stress concentration of wall corner is positively correlated with the tunnel span. The contact stress on both sides of the mushroom head and the lower section is negatively correlated with the tunnel height.
(4) The deformation control effect of DSH method is better, but the construction is slow and the cost is high. The method in this project with higher efficiency also meets the construction requirements. The stress of the arch foot and the corner is large, and the traditional theoretical calculation results are small. The design strength should be improved in engineering design, and the corner can be rounded to weaken the stress concentration. There is a possibility of excessive deflection towards the tunnel in the middle of the side wall of the lower section, and monitoring should be strengthened in the project.

Despite the achievements in numerical simulation and theoretical analysis, the scope of this study is primarily centered on specific geological conditions and engineering scenarios. The generalizability of the findings requires additional substantiation. Furthermore, existing models fall short in accurately depicting the load patterns of complex cross-sections, such as those with a mushroom shape. Future research endeavors should focus on exploring and developing more appropriate models to precisely characterize the load distribution and mechanical behavior of such intricate cross-sections. This advancement will contribute to providing a more reliable theoretical underpinning for relevant engineering designs.

ACKNOWLEDGEMENTS

This study was financially supported by the National Key R&D Program of China (Grant No.2021YFB2600900), National Natural Science Foundation of China (Grant No.52378418), Chongqing Technology Innovation and Application Development Project (CSTB2022TIAD-KPX010) and Technical Development (Entrustment) Contract of the Chongqing to Qianjiang Railway Project, Section 2, Project Management Office, China Railway 14th Bureau (CR14-DS-YQTL-[2022]-0022), and these supports are gratefully acknowledged.

REFERENCES

[1] Chen Ziquan, He Chuan, Yang Wenbo, et al. Impacts of geological conditions on instability causes and mechanical behavior of large-scale tunnels: A case study from the Sichuan–Tibet highway, China[J]. Bulletin of Engineering Geology and the Environment, 2020, 79: 3667-3688. https://doi.org/10.1007/s10064-020-01796-w

[2] Chen Ziquan, He Chuan, Xu Guowen, et al. A case study on the asymmetric deformation characteristics and mechanical behavior of deep-buried tunnel in phyllite[J]. Rock Mechanics and Rock Engineering, 2019, 52: 4527-4545. https://doi.org/10.1007/s00603-019-01836-2

[3] Xu Guowen, He Chuan, Wang Jun, et al. Study on the mechanical behavior of a secondary tunnel lining with a yielding layer in transversely isotropic rock stratum[J]. Rock Mechanics and Rock Engineering, 2020, 53: 2957-2979. https://doi.org/10.1007/s00603-020-02107-1

[4] Do Trong Nhan, Wu Jianhong. Simulation of the inclined jointed rock mass behaviors in a mountain tunnel excavation using DDA[J]. Computers and Geotechnics, 2020, 117: 103249. https://doi.org/10.1016/j.compgeo.2019.103249

[5] Yang Wenbo, Jiang Yajun, Gu Xiaoxu, et al. Deformation mechanism and mechanical behavior of tunnel within contact zone: a case study[J]. Bulletin of Engineering Geology and the Environment, 2021, 80(7): 5657-5673. https://doi.org/10.1007/s10064-021-02255-w

[6] Sabagh Mehdi, Abbas Ghalandarzadeh. Centrifugal modeling of continuous shallow tunnels at active normal faults intersection[J]. Transportation Geotechnics, 2020, 22: 100325. https://doi.org/10.1016/j.trgeo.2020.100325

[7] Ghadimi Chermahini, A., and H. Tahghighi. Numerical finite element analysis of underground tunnel crossing an active reverse fault: a case study on the Sabzkouh segmental tunnel[J]. Geomechanics and Geoengineering, 2019, 14.3: 155-166. https://doi.org/10.1080/17486025.2019.1573323

[8] Melissianos Vasileios E., Laurentiu Danciu, Dimitrios Vamvatsikos, et al. Fault displacement hazard estimation at lifeline–fault crossings: A simplified approach for engineering applications[J]. Bulletin of Earthquake Engineering, 2023, 21(10): 4821-4849. https://doi.org/10.1007/s10518-023-01710-1

[9] Kou Hao, He Chuan, Yang Wenbo, et al. Asymmetric deformation characteristics and mechanical behavior for tunnels in soft-hard inclined contact strata under high geo-stress: a case study[J]. Bulletin of Engineering Geology and the Environment, 2022, 81(7): 289. https://doi.org/10.1007/s10064-022-02784-y

[10] Vazaios Ioannis, Nicholas Vlachopoulos, M. S. Diederichs. Mechanical analysis and interpretation of excavation damage zone formation around deep tunnels within massive rock masses using hybrid finite–discrete element approach: case of Atomic Energy of Canada Limited (AECL) Underground Research Laboratory (URL) test tunnel[J]. Canadian Geotechnical Journal, 2019, 56(1): 35-59. https://doi.org/10.1139/cgj-2017-0578

[11] Liu Zhe. Study on the mechanical behavior of double primary support of soft rock tunnel under high ground stresses and large deformation[J]. Advances in Civil Engineering, 2020, 2020: 1-9. https://doi.org/10.1155/2020/8832797

[12] Chen Ziquan, He Chuan, Xu Guowen, et al. Supporting mechanism and mechanical behavior of a double primary support method for tunnels in broken phyllite under high geo-stress: a case study[J]. Bulletin of Engineering Geology and the Environment, 2019, 78: 5253-5267. https://doi.org/10.1007/s10064-019-01479-1

[13] Yu Wei, Wang Bo, Zi Xin, et al. Effect of prestressed anchorage system on mechanical behavior of squeezed soft rock in large-deformation tunnel[J]. Tunnelling and Underground Space Technology, 2023, 131: 104782. https://doi.org/10.1016/j.tust.2022.104782

[14] Wang Zhichao, Cai Yuancheng, Xie Yongli, et al. Laboratory study on mechanical behavior of hollow π-type steel–concrete composite support in loess tunnel[J]. Tunnelling and Underground Space Technology, 2023, 141: 105280. https://doi.org/10.1016/j.tust.2023.105280

[15] Xu Zilong, Chen Jianxun, Luo Yanbing, et al. Geomechanical model test for mechanical properties and cracking features of Large-section tunnel lining under periodic temperature[J]. Tunnelling and Underground Space Technology, 2022, 123: 104319. https://doi.org/10.1016/j.tust.2021.104319

[16] Luo Yong. Influence of water on mechanical behavior of surrounding rock in hard-rock tunnels: an experimental simulation[J]. Engineering Geology, 2020, 277: 105816. https://doi.org/10.1016/j.enggeo.2020.105816

[17] Zhang Heng, Zhang Gang, Pan Yingdong, et al. Experimental study on the mechanical behavior and deformation characteristics of lining structure of super-large section tunnels with a small clearance[J]. Engineering Failure Analysis, 2022, 136: 106186. https://doi.org/10.1016/j.engfailanal.2022.106186

[18] Yang Fong, Cao Shengrong, Qin Gan. Mechanical behavior of two kinds of prestressed composite linings: A case study of the Yellow River Crossing Tunnel in China[J]. Tunnelling and Underground Space Technology, 2018, 79: 96-109. https://doi.org/10.1016/j.tust.2018.04.036

[19] Wang Shimin, Ruan Lei, Shen Xingzhu, et al. Investigation of the mechanical properties of double lining structure of shield tunnel with different joint surface[J]. Tunnelling and Underground Space Technology, 2019, 90: 404-419. https://doi.org/10.1016/j.tust.2019.04.011

[20] Yang Kai, Yan Qixiang, Zhang Chuan. Three-dimensional mesoscale numerical study on the mechanical behaviors of SFRC tunnel lining segments[J]. Tunnelling and Underground Space Technology, 2021, 113: 103982. https://doi.org/10.1016/j.tust.2021.103982

[21] de Andrade, Guilherme G., Antonio D. de Figueiredo, et al. Experimental and numerical investigation of flexural behavior of precast tunnel segments with hybrid reinforcement[J]. Tunnelling and Underground Space Technology, 2024, 154: 106094. https://doi.org/10.1016/j.tust.2024.106094

[22] González-Nicieza C, Álvarez-Vigil A E, Menéndez-Díaz A, et al. Influence of the depth and shape of a tunnel in the application of the convergence–confinement method[J]. Tunnelling and Underground Space Technology, 2008, 23(1): 25-37. https://doi.org/10.1016/j.tust.2006.12.001

[23] Cai Xin, Yuan Jifeng, Zhou Zilong, et al. Effects of hole shape on mechanical behavior and fracturing mechanism of rock: Implications for instability of underground openings[J]. Tunnelling and Underground Space Technology, 2023, 141: 105361. https://doi.org/10.1016/j.tust.2023.105361

[24] Liu Xian, Ye Yuhang, Liu Zhen, et al. Mechanical behavior of Quasi-rectangular segmental tunnel linings: First results from full-scale ring tests[J]. Tunnelling and Underground Space Technology, 2018, 71: 440-453. https://doi.org/10.1016/j.tust.2017.09.019

[25] Huang Zhen, Zhang Chenlong, Ma Shaokun, et al. Study of the mechanical behaviour and damage characteristics of three new types of joints for fabricated rectangular tunnels using a numerical approach[J]. Tunnelling and Underground Space Technology, 2021, 118: 104184. https://doi.org/10.1016/j.tust.2021.104184

[26] Nguyen, Tien Tai, Anh Ngoc Do. Influence of interior column on the behaviour of quasi-rectangular tunnel[J]. Journal of Mining and Earth Sciences, 2024, 65(2): 22-29. DOI:10.46326/JMES.2024.65(2).03

[27] A.Z. Lu, H.Y. Chen, Y. Qin, et al. Shape optimisation of the support section of a tunnel at great depths[J]. Computers and Geotechnics, 2014, 61: 190-197. https://doi.org/10.1016/j.compgeo.2014.05.011